DEPARTMENT OF THE INTERIOR
U.S. GEOLOGICAL SURVEY

Geochemical investigations and assessment of anomalous radioactivity at Ba'gham, Kingdom of Saudi Arabia

by

J. S. Stuckless[1/], J. E. Quick, and G. VanTrump, Jr.

Open-File Report 84-850

Prepared for the Ministry of Petroleum and Mineral Resources, Deputy Ministry for Mineral Resources, Jiddah, Kingdom of Saudi Arabia

This report is preliminary and has not been reviewed for conformity with U.S. Geological Survey editorial standards and stratigraphic nomenclature.

1/ U.S. Geological Survey, Denver, CO 80225

1984

CONTENTS

ILLUSTRATIONS

Page

TABLES

GEOCHEMICAL INVESTIGATIONS AND ASSESSMENT OF ANOMALOUS RADIOACTIVITY AT BA'GHAM, KINGDOM OF SAUDI ARABIA

by
J. S. Stuckless[1]/, J. E. Quick,
and G. VanTrump, Jr.[1]/

ABSTRACT

Examination of anomalously radioactive areas near Ba'gham, Kingdom of Saudi Arabia, shows that most of the radioactivity is due to thorium and that the volume of rock with very high concentrations of thorium is small. All significant anomalies occur within a 600-Ma-old postorogenic granite that is similar in terms of major-element chemistry to other postorogenic granites of the northern Arabian Shield, but is more highly evolved in terms of trace elements. Available evidence suggests, at least in part, that the trace-element concentrations reflect a hydrothermal alteration event. Data for several trace elements define a halo around a likely center for hydrothermal alteration. Identification of similar halos may prove useful in the search for larger deposits of thorium, uranium, rare-earth elements, and niobium associated with the postorogenic granites.

INTRODUCTION

During field mapping of the Ghazzalah quadrangle, sheet 26/41 A (Quick, 1983), a large area of anomalous radioactivity was noted near Ba'gham (fig. 1). Subsequent ground traverses confirmed the existence of several small but highly radioactive localities within a postorogenic alkali-feldspar granite. Material from these localities was collected for analysis. In addition, samples were collected from apparently unmineralized portions of the alkali-feldspar granite as well as an earlier two-feldspar granite. These samples were taken in order to compare the geochemical signature of the granites associated with the anomalous radioactivity with the general geochemical signature of the postorogenic granites of the northeastern Arabian Shield (Stuckless, VanTrump, and others, 1982).

Mathews (1978) has noted that peralkaline granites are particularly favorable hosts for anomalous concentrations of uranium. Geologic descriptions also show that thorium and rare-earth-element deposits are usually associated with peralkaline granites and syenites (Staatz and others, 1980). Most of the thorium and rare-earth deposits of the United States are also associated with carbonatites - for example, Mountain Pass, California (Olson and others, 1954); the Powderhorn area, Colorado (Olson and others, 1977); and the Wet Mountains, Colorado (Armbrustmacher, 1979). However, deposits such as Bokan Mountain, Alaska, seem to be entirely igneous and free of carbonate minerals (Staatz and others, 1980).

1/ U.S. Geological Survey, Denver, Colorado 80225

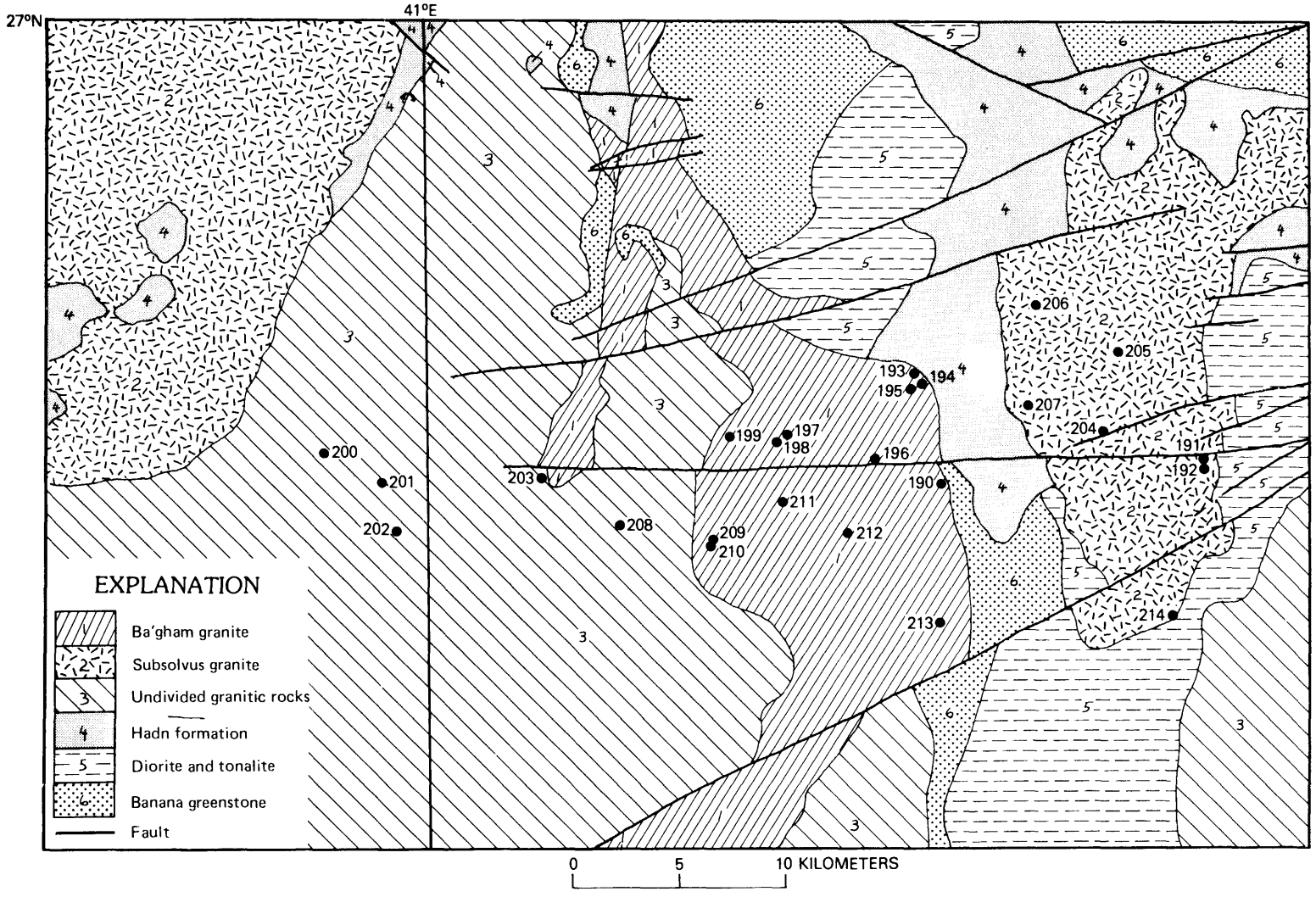

Figure 1.—Map showing location of study area, generalized geology (Quick, 1983), and sample localities. Samples are restricted to three bodies of granite: (1) a large body of undivided granitic rocks previously mapped by Quick (1983) as magnetite syenogranite; (2) the Ba'gham granite; and (3) the body of subsolvus granite that was mapped as the Jufayfah syenogranite (Quick, 1983) and lies to the east of the Ba'gham granite.

Elliott (1983) has noted that the postorogenic alkali-feldspar granites of the Arabian Shield are chemically similar to other specialized granites that are associated with niobium, tantalum, and rare-earth-element deposits. Anomalous contents of thorium and rare-earth elements have been noted in peralkaline postorogenic granites of the northern Arabian Shield (Harris and Marriner, 1980; Stuckless, Knight, and others, 1982). Therefore, abundance of niobium and yttrium, that are geochemically similar to the rare-earth elements (Felsche and Herrman, 1978), were determined for all of the granite samples as a check for regional enrichments in these suites of rare elements.

This investigation was performed in connection with reconnaissance geologic mapping of the Ghazzalah quadrangle (sheet 26/41 A) as part of the work agreement between the Ministry of Petroleum and Mineral Resources, Kingdom of Saudi Arabia, and the U.S. Geological Survey for systematic mapping in western Saudi Arabia. The results given in this report are part of the study of petrogenesis and mineral potential of the granitic rocks of the Arabian Shield.

The classification of plutonic rocks used in this study is that recommended by the International Union of Geological Sciences (IUGS) Subcommission on the Systematics of Igneous Rocks (Streckeisen, 1976). The definitions of Shand (1951) are used to subdivide the rocks on the basis of alumina saturation. Decay constants and isotopic ratios used are those recommended by the IUGS Subcommission on Geochronology (Steiger and Jager, 1977).

GEOLOGIC SETTING

The Jibal Ba'gham radioactive anomalies are located within an elongate body of granite that was mapped as the Ba'gham intrusive complex (Quick, 1983). A geologic map of the complex south of lat 27°00'N. and surrounding rocks is presented in figure 1. The complex is composed of a main body of arfvedsonite-bearing alkali-feldspar granite and a narrow, eastern rim of granophyre; these rocks crop out in a bifurcating belt along the eastern margin of a large mass of magnetite syenogranite. To the east, the Ba'gham complex is separated from the Jufayfah syenogranite (Quick, 1983; Stoeser, 1984) by a septum composed of hornblende quartz diorite, tonalite, and two sequences of volcanosedimentary rocks named the Hadn formation (Chevremont, 1982; Stoeser, unpub. data, 1984) and the Banana greenstone (Quick, 1983). All of the above rocks are broken by a northeast-trending system of high-angle faults that appear to have a significant right- lateral component of slip (Quick, 1983).

The hornblende quartz diorite, tonalite, and volcanosedimentary rocks constitute the country rocks into which the Ba'gham intrusive complex and two syenogranite bodies were emplaced. The Banana greenstone is composed of intermediate volcanic and subvolcanic rocks and minor interbedded marble, which are metamorphosed to greenschist-facies assemblages. Volcanic rocks mainly range in composition from basalt to

adnesite, and subvolcanic rocks consist of diorite and diabase. The Banana greenstone is interpreted to be the oldest unit in the quadrangle (Quick, 1983) and is intruded by hornblende quartz diorite and tonalite. These rocks are, in turn, unconformably overlain by rhyolitic to dacitic volcanic rocks and continental sedimentary rocks of the Hadn formation. In contrast to the Banana greenstone, the volcanosedimentary rocks of the Hadn formation are only incipiently metamorphosed. The unconfirmity is regional in extent (Chevremont, 1982; Quick, 1983; Kellogg, 1983), and the contrasting metamorphic grade and volcanic style of the Hadn formation and Banana greenstone suggest that it marks the end of a major hiatus in the history of the northern Arabian Shield.

The Ba'gham intrusive complex and the two syenogranite bodies intrude the Hadn formation and are therefore significantly younger than the hornblende quartz diorite and tonalite. There are no mutual contacts between the Ba'gham intrusive complex (shown as Ba'gham granite on fig. 1) and the Jufayfah syenogranite (shown as subsolvus granite on fig.1), and their relative ages cannot be determined in the field. The magnetite syenogranite (included with undivided granitic rocks on fig. 1) was originally mapped by Quick (1983) as a pre-Hadn intrusive rock on the basis of the occurrence of syenogranite clasts in the Hadn formation. As a result, the magnetite syenogranite was mapped as a separate pluton genetically unrelated to the Ba'gham intrusive complex. Subsequent mapping in the adjacent quadrangle to the west (26/40 B; Quick, 1984) has located contacts where the same body of magnetite syenogranite clearly intrudes the Hadn formation. Therefore, it now appears more likely that the magnetite syenogranite and the Ba'gham granite could be related. The contact between magnetite syenogranite and the Ba'gham intrusive complex is difficult to locate in the field and, in most places, appears to be gradational, suggesting that the two units are cogenetic. This hypothesis is further supported by the geometry of the two granites, which suggests that the Ba'gham intrusive complex is actually a peralkaline rim on the east side of a large, zoned pluton.

Previous isotopic investigations place some constraints on the absolute ages of events in the area. The Banana greenstone is tentatively correlated with the Hulayfah formation (Quick, 1983), which crops out approximately 150 km to the south and is estimated to be older than 700 m.y. on the basis of K-Ar age dating (Delfour, 1977). A similar age for the Banana greenstone would be consistent with rubidium/strontium isotopic data reported by R. J. Fleck (written commun., 1982) that suggests and age of 630 m.y. for tonalite bodies that crop out about 10 to 20 km north of the Ba'gham area. Fleck (written commun., 1982) has also reported preliminary rubidium/ strontium isotopic data for the Hadn formation and the Jufayfah syenogranite. The data sets for both of these units display considerable scatter on an Rb/Sr evolution diagram, suggesting that the Rb/Sr isotopic systematics of both units have been greatly disturbed. A least-squares fit to the data for the Hadn volcanic rocks yields a "best-fit"

isochron corresponding to an age of about 613 m.y. and an initial $^{87}Sr/^{86}Sr$ of 0.7034. This data set, unfortunately, does not define a sufficiently precise array on a Rb/Sr evolution diagram to assign an unequivocal age to the Hadn.

ANALYTICAL PROCEDURES

Major-element concentrations (table 1) were determined by high-precision X-ray fluorescence (Taggart and others, 1982) on 0.8-g splits of fused sample powder. Results are precise and accurate within ±2 percent of the amount present (2 sigma) for abundances greater than 1 percent absolute. A fourth digit is reported for SiO_2 and Al_2O_3 that is not significant for any single sample, but may be significant in a statistical treatment of the entire data set (A. T. Miesch, oral commun., 1980). Values for MgO, P_2O_5, and MnO that are below the limits of detection were arbitrarily assigned a value of one-half the limit of detection for purposes of statistical and normative calculations.

Radium-equivalent uranium (RaeU), thorium (eTh), and potassium (eK) contents (table 2) were determined by sealed-can gamma-ray spectrometry (Bunker and Bush, 1966, 1967) on approximately 600 g of coarsely crushed material (-32 mesh). The prefix "e" is used to distinguish values determined by this method. RaeU is not a direct measure of uranium, but rather a measure of the amount of uranium needed for secular equilibrium between ^{238}U and ^{226}Ra. Although eTh is not determined directly from thorium, disequilibrium within the thorium decay chain is unlikely. Therefore, eTh is used as a true measure of thorium. Precision for eTh and RaeU is better than ± the quantity (2 percent of the amount reported plus 0.1 ppm absolute). The eK value obtained by gamma-ray spectrometry is a direct measure of potassium that is precise to within ± the quantity (2 percent of the amount reported plus 0.03 percent absolute). Accuracies for the gamma-ray technique are generally equal to precisions except where relative proportions of uranium, thorium, and potassium deviate markedly from normal (approximately by more than a factor of 10 from K:U:Th of 10,000:1:3), in which case accuracy for the element with relatively low abundance is decreased.

Uranium (U) and thorium (Th) contents (table 2) were determined by the delayed-neutron technique (Millard, 1976) on 8- to 10-g splits of sample powder. Accuracies for reported concentrations are dependent on counting statistics that are dependent on both concentrations and relative proportions of uranium and thorium. Uranium contents obtained for this study are accurate to within ±4 percent of the amount reported for all samples (2 sigma). Thorium contents for non- mineralized samples are generally accurate to within ±16 percent of the amount reported and to within ±4 percent of the amount reported for the mineralized samples (2 sigma).

Table 1.--Chemical and normative analyses for granitic samples from Ba'gham, Kingdom of Saudi Arabia

[Analyses in weight percent. Letter symbols refer to hypersolvus (H) and subsolvus (S) granites. D.I. is the differentiation index of Thornton and Tuttle, 1960. Fe_2O_3 and FeO calculated from the total iron assuming 2/3 of the iron is present as FeO. LOI is loss on ignition at 920°C. Analyst: A.J. Bartel]

Symbol	155190 H	155191 S	155192 S	155193 H	155196 H	155198 H	155201 H	155202 H	155203 H	155204 S
SiO_2	75.43	73.93	74.18	75.47	75.29	76.61	75.31	75.91	74.05	73.58
Al_2O_3	11.35	13.06	13.22	10.72	11.04	11.11	11.84	12.51	12.11	13.25
Fe_2O_3	0.96	0.56	0.57	1.22	1.08	0.86	0.67	0.39	0.74	0.56
FeO	1.73	1.01	1.02	2.19	1.94	1.54	1.21	0.70	1.33	1.01
MgO	<0.10	0.29	0.29	<0.10	<0.10	<0.10	<0.10	<0.10	0.15	0.26
CaO	0.30	0.88	0.89	0.17	0.21	0.25	0.35	0.59	0.75	0.96
Na_2O	3.02	3.49	3.52	2.87	3.71	3.19	3.56	3.55	3.20	3.55
K_2O	4.92	4.78	4.90	4.53	4.50	4.51	4.53	4.70	4.87	4.83
LOI	0.63	0.60	0.56	0.62	0.42	0.80	0.49	0.49	1.11	0.44
TiO_2	0.12	0.21	0.21	0.16	0.16	0.13	0.11	0.06	0.19	0.21
P_2O_5	<0.05	<0.05	<0.05	<0.05	<0.05	<0.05	<0.05	<0.05	<0.05	<0.05
MnO	0.06	0.03	0.03	<0.02	0.04	<0.02	<0.02	<0.02	<0.02	0.03
ZrO_2	0.07	0.02	0.02	0.33	0.05	0.14	0.05	0.01	0.05	0.02
Total	98.66	98.88	99.43	98.36	98.50	99.22	98.20	98.99	98.57	98.72
Normative minerals										
Q	37.80	32.94	32.34	40.30	35.56	39.60	36.44	35.946	34.80	31.96
C	0.57	0.60	0.56	0.85		0.58	0.50	0.564	0.26	0.49
Z	0.11	0.03	0.03	0.50	0.08	0.21	0.08	0.015	0.08	0.03
OR	29.47	28.57	29.12	27.22	26.10	26.86	27.26	28.056	29.20	28.91
AB	25.90	29.87	29.96	24.69	31.87	27.21	39.67	30.345	27.47	30.43
AN	1.38	4.28	4.31	0.72	0.18	1.12	1.64	2.825	3.64	4.69
WO					0.31					
EN	0.13	0.73	0.73	0.13	0.13	0.13	0.13	0.126	0.38	0.66
FS	2.33	1.11	1.12	2.82	2.52	1.94	1.54	0.896	1.56	1.11
MT	1.41	0.82	0.83	1.79	1.58	1.25	0.99	0.571	1.08	0.82
IL	0.23	0.40	0.40	0.31	0.31	0.25	0.21	0.115	0.37	0.40
AP	0.05	0.05	0.05	0.05	0.05	0.05	0.05	0.048	0.05	0.05
Total	99.36	99.40	99.44	99.37	99.58	99.20	99.50	99.507	98.88	99.56
Salic	95.22	96.28	96.32	94.28	94.68	95.58	96.59	97.751	95.44	96.51
Femic	4.14	3.11	3.12	5.10	4.90	3.62	2.92	1.756	3.43	3.04
D.I.	93.17	91.37	91.42	92.20	94.42	93.67	94.38	94.35	91.46	91.30

Table 1.--Chemical and normative analyses for granitic samples from Ba'gham, Kingdom of Saudi Arabia--Continued

Symbol	155205 S	155206 S	155207 S	155208 H	155209 H	155210 H	155211 H	155213 H	155214 S
SiO_2	73.54	74.00	73.34	74.04	74.52	69.29	74.93	76.07	75.66
Al_2O_3	13.22	13.41	13.11	12.63	11.82	14.21	11.46	11.27	12.69
Fe_2O_3	0.58	0.60	0.66	0.81	0.93	0.99	1.00	0.76	0.42
FeO	1.04	1.07	1.19	1.45	1.68	1.78	1.79	1.36	0.76
MgO	0.31	0.29	0.33	<0.10	<0.10	0.26	<0.10	0.10	<0.10
CaO	0.82	0.85	0.69	0.28	0.45	1.02	0.25	0.31	0.27
Na_2O	3.52	3.40	3.27	3.59	3.85	5.16	3.91	3.22	3.33
K_2O	4.80	4.85	4.96	5.06	4.80	4.64	4.57	4.63	4.94
LOI	0.74	0.54	1.15	0.66	0.17	0.54	0.39	0.65	0.73
TiO_2	0.22	0.21	0.22	0.16	0.20	0.33	0.14	0.11	0.11
P_2O_5	<0.05	0.05	<0.05	<0.05	<0.05	0.06	<0.05	<0.05	<0.05
MnO	0.04	0.07	0.03	<0.02	0.03	0.05	0.04	0.05	0.02
ZrO_2	0.02	0.02	0.02	0.06	0.07	0.06	0.12	0.07	0.02
Total	98.86	99.36	98.99	98.82	98.59	98.39	98.67	98.62	99.02
Normative minerals									
Q	32.37	33.18	33.14	32.73	32.55	19.08	33.67	38.55	36.73
C	0.80	1.15	1.17	0.80				0.45	1.44
Z	0.03	0.03	0.03	0.09	0.11	0.09	0.18	0.11	0.03
OR	28.69	28.84	29.61	30.26	28.77	27.87	27.37	27.74	29.48
AB	30.13	28.96	27.95	30.74	33.04	44.38	33.53	27.63	28.46
AN	3.98	3.92	3.33	1.27	0.81	1.94	0.22	1.43	1.22
WO					0.55	1.17	0.38		
EN	0.78	0.73	0.83	0.13	0.13	0.66	0.13	0.25	0.13
FS	1.16	1.27	1.34	1.78	2.07	2.04	2.35	1.81	0.91
MT	0.84	0.87	0.97	1.18	1.37	1.46	1.46	1.11	0.61
IL	0.42	0.40	0.42	0.31	0.38	0.64	0.27	0.21	0.21
AP	0.05	0.12	0.05	0.05	0.05	0.14	0.05	0.05	0.05
Total	99.25	99.46	98.84	99.33	99.83	99.46	96.61	99.34	99.26
Salic	96.00	96.07	95.23	95.89	95.27	93.35	94.98	95.90	97.36
Femic	3.25	3.39	3.61	3.44	4.56	6.10	4.63	3.44	1.90
D.I.	91.19	90.98	90.71	93.73	94.36	91.32	94.57	93.92	94.67

Table 2.--Locations and trace-element contents and ratios for granitic samples from Ba'gham, Kingdom of Saudi Arabia [Analysts: U and Th, R. B. Vaughn, RaeU, eth, and ek, C. A. Bush; Rb, Sr, Y, Zr, and Nb, J. S. Stuckless.]

Sample	Latitude (north)	Longitude (east)	U (ppm)	RaeU (ppm)	Th (ppm)	eTh (ppm)	K (wt %)	eK (wt %)	Rb (ppm)	Sr (ppm)
155190	26°55'23"	40°54'22"	21.5	19.7	72.1	75.9	4.08	4.11	375	28.9
155191	26°55'30"	40°51'25"	8.0	4.9	31.2	31.1	3.97	4.16	250	89.3
155192	26°55'30"	40°51'25"	10.2	9.2	30.7	31.0	4.07	4.09	257	88.4
155193	26°56'28"	40°54'40"	38.7	32.4	69.4	70.9	3.76	3.75	531	28.2
155196	26°55'34"	40°55'05"	14.8	14.1	30.5	34.5	3.74	3.75	412	9.0
155198	26°55'48"	40°56'10"	17.3	16.0	142.0	144.0	3.74	3.86	370	15.0
155201	26°55'26"	41°00'32"	7.6	7.7	13.8	20.0	3.76	3.71	159	10.6
155202	26°54'54"	41°00'22"	6.9	6.4	19.7	19.7	3.90	4.09	175	12.7
155203	26°55'26"	40°58'44"	5.8	5.2	16.3	17.6	4.04	3.95	104	28.0
155204	26°55'55"	40°52'34"	12.6	10.3	35.3	29.5	4.01	4.11	275	87.8
155205	26°56'42"	40°52'26"	7.9	5.9	33.8	27.4	3.98	3.96	243	90.4
155206	26°57'11"	40°53'17"	12.8	10.7	35.7	30.2	4.03	4.05	271	88.8
155207	26°56'10"	40°53'20"	13.3	12.0	31.0	30.4	4.12	4.17	267	97.5
155208	26°54'58"	40°57'54"	5.4	4.9	16.6	18.0	4.20	4.27	143	33.4
155209	26°54'43"	40°56'53"	5.7	5.0	31.6	33.2	3.98	4.02	231	17.5
155210	26°54'43"	40°56'53"	6.2	5.7	14.2	16.1	3.85	4.04	204	52.0
155211	26°55'12"	40°56'06"	21.7	19.7	31.6	36.9	3.79	3.80	348	13.6
155213	26°54'00"	40°54'22"	12.0	8.2	21.2	23.3	3.84	3.95	271	13.1
155214	26°53'56"	40°51'43"	4.7	4.2	33.3	36.3	4.10	4.17	260	47.7

Table 2.--Locations and trace-element contents and ratios for granitic samples from Ba'gham, Kingdom of Saudi Arabia -- [Continued]

Sample	Y (ppm)	Zr (ppm)	Nb (ppm)	eTh/ U	eK/ U	eTh/ eK	K/ Rb	Rb/ Sr	RaeU/ U	Al/ (Na+K)	Al/ (Na+K+Ca)
155190	238.0	529	181	3.53	.19	18.47	109	12.98	.92	1.10	1.05
155191	40.8	169	37	3.89	.52	7.48	159	2.80	.61	1.20	1.04
155192	43.4	172	35	3.04	.40	7.58	158	2.91	.90	1.19	1.04
155193	300.0	2,450	507	1.83	.10	18.91	71	18.83	.84	1.11	1.08
155196	142.0	349	128	2.33	.25	9.20	91	45.78	.95	1.01	.97
155198	204.0	1,060	213	8.32	.22	37.31	101	24.67	.92	1.10	1.05
155201	95.9	370	31	2.63	.49	5.39	236	15.00	1.01	1.10	1.04
155202	37.5	108	30	2.86	.59	4.82	223	13.78	.93	1.14	1.04
155203	76.0	354	26	3.03	.68	4.46	388	3.71	.90	1.15	1.02
155204	44.0	178	38	2.34	.33	7.18	146	3.13	.82	1.20	1.03
155205	40.3	173	31	3.47	.50	6.92	164	2.69	.75	1.20	1.06
155206	46.2	179	42	2.36	.32	7.46	149	3.05	.84	1.24	1.08
155207	46.7	179	36	2.29	.31	7.29	154	2.74	.90	1.22	1.09
155208	57.2	422	59	3.33	.79	4.22	294	4.28	.91	1.11	1.06
155209	90.0	482	60	5.82	.71	8.26	172	13.20	.88	1.03	.96
155210	51.1	433	38	2.60	.65	3.99	189	3.92	.92	1.05	.92
155211	189.0	919	189	1.70	.18	9.71	109	25.59	.91	1.01	.97
155213	176.0	500	114	1.94	.33	5.90	142	20.69	.68	1.09	1.04
155214	51.7	150	48	7.72	.89	8.71	158	5.45	.89	1.17	1.12

Concentrations for rubidium (Rb), strontium (Sr), yttrium (y), niobium (Nb), and zirconium (Zr) were determined by X-ray fluorescence on loose, finely ground (-200 mesh) sample powders. Results (table 2) are estimated to be precise to within ±10 percent of the amount reported (2 sigma). Mineralized samples were found to have a significant interference from thorium. Results were judged to be unreliable and therefore are not reported.

Normative mineralogy was calculated according to the methods described by Stuckless and VanTrump (1979). Statistical methods and formulae used are described by VanTrump and Niesch (1977). Means and standard deviations for trace-element contents were calculated from the logarithms of the data and are reported as antilog values (table 3).

Rubidium and strontium concentrations and the isotopic composition of strontium were determined on separate dissolutions that were spiked with tracers of ^{87}Rb and ^{84}Sr. Replicate analyses of granitic samples with comparably high Rb/Sr ratios and mineralogically inhomogeneous $^{87}Sr/^{86}Sr$ values indicate an analytical accuracy of ±1.75 percent for the $^{87}Rb/^{86}Sr$ ratio and 0.035 percent for the $^{87}Sr/^{86}Sr$ values (2 sigma). Reported isotopic analyses (table 4) have been adjusted to a $^{88}Sr/^{86}Sr$ value of 0.1194. The methods of York (1969) were used to obtain best-fit lines for isochrons, and results are reported at the 95-percent level of confidence.

RESULTS AND DISCUSSIONS

Petrography

Ba'gham intrusive complex

Most of the Ba'gham intrusive complex is composed of coarse-grained dark-gray-weathering granite. The primary mineralogy of this rock is a hypidiomorphic-granular inter-growth of 50 to 70 percent microcline microperthite, 30 to 45 percent quartz, 5 to 10 percent arfvedsonite, minor amounts of equant opaque minerals and zircon, and trace amounts of yellow biotite. The presence of arfvedsonite suggests that the granite is peralkaline in composition. The mineralogy and textures along the west margin of this granite, in the vicinity of the radiometric anomalies, preserve a record of late-stage magmatic recrystallization and oxidation. Ellipsoidal pegmatitic segregations, as much as 20 cm in diameter, are locally present and probably crystallized from late-stage, volatile-rich fluids. The rock is cut by ubiquitous hematite veins and weathers red due to pervasive hematite staining. Ferromagnesian minerals are replaced by dark, hematite-rich clots. Hematite-rich veinlets (10-100 mm wide) are present along grain boundaries and within microcline grains parallel to exsolution lamellae. Locally, incipient protoclastic texture is evident; interstices and grain boundaries are occupied by fragments of crushed primary grains and secondary hematite.

Table 3.--Mean and standard deviation for granitic samples from the Ba'gham area compared to other postorogenic granites of the northeastern Arabian Shield and average granite

[Oxide concentrations are in weight percent; trace-element contents are in parts per million. Average granite values from Krauskopf (1967) and Stuckless and VanTrump (1982) with major elements converted to oxides and normalized to 100 percent. Values for the northeastern Shield from Stuckless, Knight and others (1982).]

	All Ba'gham		Hypersolvus		Subsolvus		NE Shield		Average
	Mean	S.D.	Mean	S.D.	Mean	S.D.	Mean	S.D.	granite
SiO_2	74.48	1.58	74.74	1.88	74.03	.78	74.64	3.03	72.64
Al_2O_3	12.32	.99	11.84	.95	13.14	.23	12.3	1.24	13.67
Fe_2O_3	2.26	.69	2.6	.65	1.69	.22	2.46	1.11	3.63
MgO	.15	.12	.08	.06	.26	.1	.23	.26	.25
CaO	.54	.3	.41	.25	.77	.23	.58	.51	2.1
Na_2O	3.52	.48	3.6	.6	3.44	.11	3.94	.5	3.54
K_2O	4.75	.17	4.69	.18	4.87	.07	4.79	.43	3.74
TiO_2	.17	.06	.16	.07	.2	.04	.2	.18	.36
MnO	.03	.02	.03	.02	.04	.02	.05	.03	.05
U	10.4	7.9 -4.5	11	10.4 -5.3	9.4	4.3 -2.9	5.63	4.08 -2.36	3.54
RaeU	9	7 -3.9	9.8	9.1 -4.7	7.6	4 -2.6	5.57	3.64 -2.2	--
Th	31.1	24.8 -13.8	29.7	32.8 -15.6	33.6	3 -2.7	16.3	11.4 -6.7	16.8
eTh	32	23.5 -13.5	32.8	33.2 -16.5	30.7	2.7 -2.5	16.7	11 -6.6	--
Rb	253	120 -82	249	160 -97	260	12 -11	148	75 -50	150
Sr	32.7	43.9 -18.7	19	13.6 -7.9	82.4	22.8 -17.8	29.2	41 -17	285
Y	80.8	82.2 -40.8	114	109 -55.7	44.6	4 -3.7	--	-- --	40
Zr	339	412 -186	505	565 -267	171	11 -10	370	317 -171	180
Nb	64	86 -37	86	136 -53	38	6 -5	--	-- --	20
K/Rb	156	78 -52	156	106 -63	155	6 -6	373	191 -126	--
Rb/Sr	7.74	12.4 -4.76	13.1	25.1 -7.21	3.2	.9 -.7	5.07	10.8 -3.45	--
eTh/U	3.08	1.72 -1.1	2.97	1.76 -1.1	3.27 -1.15	1.77	2.93 -.76	1.02	4.73
eTh/eK	8.01	6.03 -3.44	8.32	8.66 -4.24	13.1	1 -.9	4.12	2.7 -1.63	5
eK/U	.39	.3 -.17	.36	.35 -.18	.46	.21 -.15	.71	.52 -.3	.95
RaeU/U	.87	.1	.9	.08	.82	.11	1.01	.21	--

Table 4.--Rubidum and stronium concentrations and the isotopic composition of strontium for whole-rock granite samples from Ba'gham, Kingdom of Saudi Arabia [Analyst: K. Futa]

Sample Number	Rb (ppm)	Sr (ppm)	87Rb/86Sr	87Sr/86Sr
155190	364.2	25.83	42.41	1.0687
155192	259.8	89.59	8.451	0.77305
155196	404.0	7.30	184.7	2.2638
155198	359.0	7.16	165.3	2.1226
155204	275.3	87.88	9.138	0.77944
155205	244.3	89.94	7.924	0.76849
155206	275.5	87.17	9.218	0.78085
155208	143.2	30.54	13.72	0.81893

Amphibole has been completely replaced by intergrowths of magnetite, quartz, calcite, and potassium feldspar, but the primary amphibole morphology is preserved by trails of opaque minerals.

The granophyre on the east side of the intrusive complex is composed of about 40 to 55 percent potassium feldspar, 30 percent quartz, 10 percent albite microphenocrysts, and minor amounts of biotite and opaque minerals. The rock is typically fine grained, although locally it is porphyritic with phenocrysts of potassium feldspar and quartz as large as 15 mm.

Magnetite syenogranite

The magnetite syenogranite, like altered parts of the Ba'gham complex, is characterized by a pervasive red staining, abundant hematite-filled fractures, and the presence of small magnetite-rich clots. The rock is composed of a xenomorphic-granular intergrowth of quartz and microcline perthite. Interstices between the quartz and microcline are filled with minor plagioclase (An_{25-35}), myrmekitic intergrowths of quartz and feldspar, and clots of magnetite $\pm$ muscovite, biotite, quartz, albite, and zircon. Locally, the rock has a cataclastic texture with interstices between large, angular frag- ments from the primary minerals and by veins of secondary hematite.

Jufayfah Syenogranite

The Jufayfah syenogranite is composed of a fine- to medium-grained hypidiomorphic-granular intergrowth of 35 to 40 percent quartz, 40 percent microcline, 15 to 20 percent plagioclase (An_{25-35}), and minor amounts of biotite and opaque minerals $\pm$ green to brown hornblende. Interstitial muscovite is present in some rocks but may be a secondary phase. The potassium feldspars are partially altered to hematite, clay minerals, and muscovite, and biotite has been largely replaced by opaque minerals and chlorite. However, the effects of alteration are much less obvious in the Jufayfah syenogranite than in the magnetite syenogranite or the Ba'gham intrusive complex.

Chemistry

The average major-element compositions for the hypersolvus (the Ba'gham granite and the magnetite syenogranite) and subsolvus granites (Jufayfah syenogranite) are very similar to the average major-element composition for the postorogenic granites of the northeastern Arabian Shield (table 3). In fact, the average composition for all samples from near Ba'gham is indistinguishable from the average composition for the postorogenic granites of the northeastern Arabian Shield. Data for all but one of the granite samples from the Ba'gham area approximate the ternary minimum in the haplogranite system (fig. 2) and suggest a low partial pressure of water during most of the crystallization history. Normative feldspar compositions also

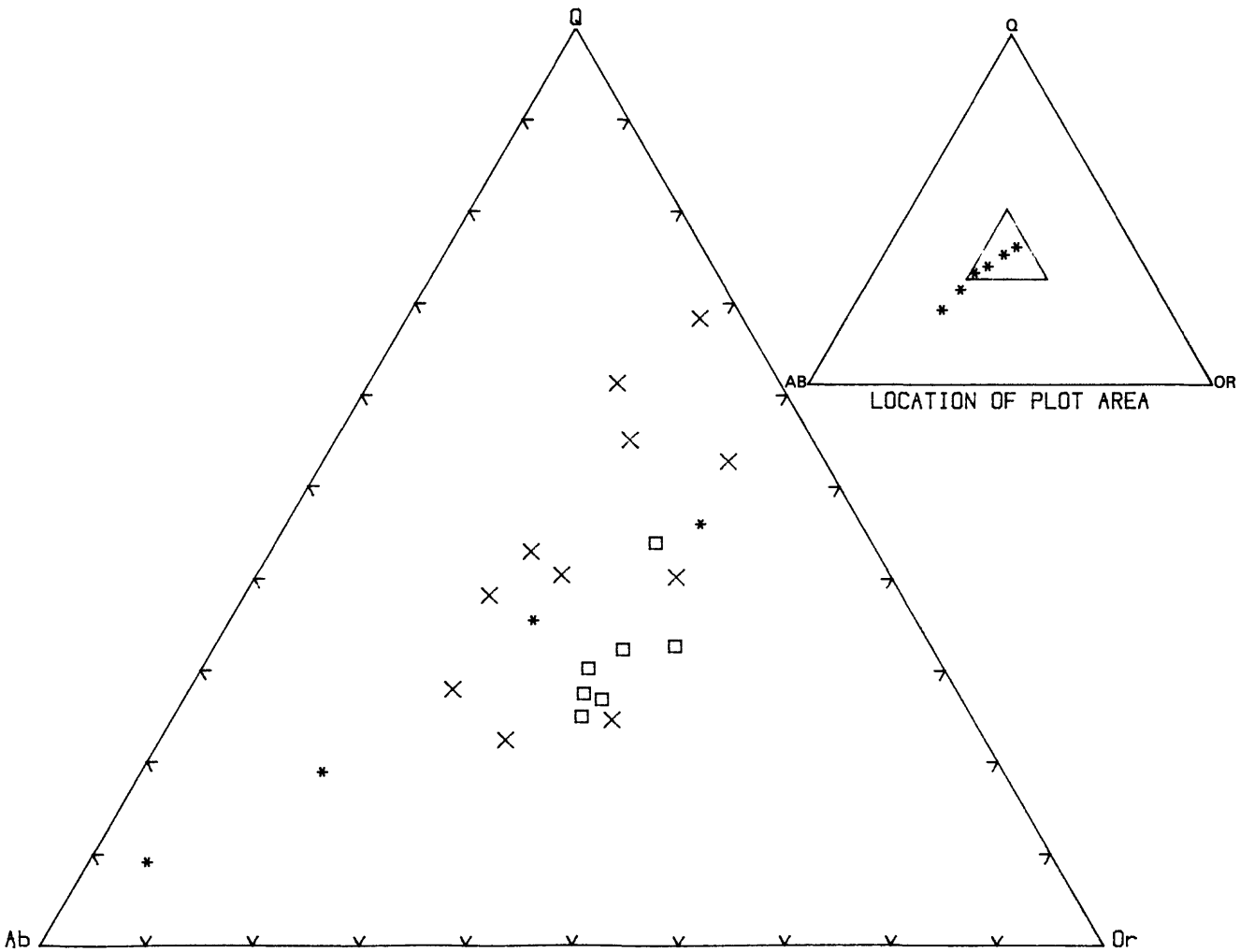

Figure 2.—Ternary diagram showing the normative composition of granitic samples from Ba'gham and the water-saturated polybaric ternary minimun (delineated by asterisks) in the system Q-Ab-Or (Tuttle and Bowen, 1958; Luth and others, 1984). Data for hypersolvus granite are shown by X and for subsolvus granite by squares.

suggest low partial pressure of water and further suggest a lower water pressure for the hypersolvus granite (fig. 3).

In contrast to the major-element compositions, the average trace-element contents show some significant differences relative to the postorogenic granites of the northeastern Arabian Shield. Both the hypersolvus and subsolvus granites exhibit significant enrichments in uranium and thorium with correspondingly high Th/K and low K/U values (table 3). In fact, compared to average granite (reported by Stuckless and VanTrump, 1982), most of the samples from the Ba'gham area are enriched in uranium and thorium relative to potassium and in uranium relative to thorium (fig. 4).

Both granites, by virtue of their much lower average K/Rb value, seem to be significantly more evolved than the average postorogenic granite. This condition could be due to a more petrogenetically evolved source region, a higher degree of differentiation, a lower degree of partial melting, or a hydrothermal overprint, all of which also increase the probability for increased contents of incompatible elements. Yttrium and niobium data are not available for the post- orogenic granites of the northeastern Arabian Shield; however, one or both of these trace elements is enriched in the granites from Ba'gham (table 3) relative to the average granite reported by Krauskopf (1967).

There are subtle chemical differences between the hypersolvus and subsolvus granites. The hypersolvus granite contains slightly less aluminum and more iron and zirconium. These differences suggest a peralkaline affinity for the hypersolvus granite; however, none of the samples is truly peralkaline, and all but four of twelve are weakly peraluminous (tables 1 and 2). This apparent degree of alumina saturation may, however, reflect minor postmagmatic alteration, because small amounts of alkali loss from low-calcium peralkaline rocks can move compositions to the peraluminous field. All of the subsolvus granites are peraluminous.

The very high average Rb/Sr value for the hypersolvus granite suggests a somewhat higher degree of petrologic evolution for this granite relative to the subsolvus granite. The hypersolvus granite also contains more yttrium and niobium. The niobium enrichment may be due in part to the peralkaline affinity of the hypersolvus granite (Elliott, 1983), but the yttrium (and presumably rare-earth-element) enrichment is again expected with a higher degree of petrologic evolution.

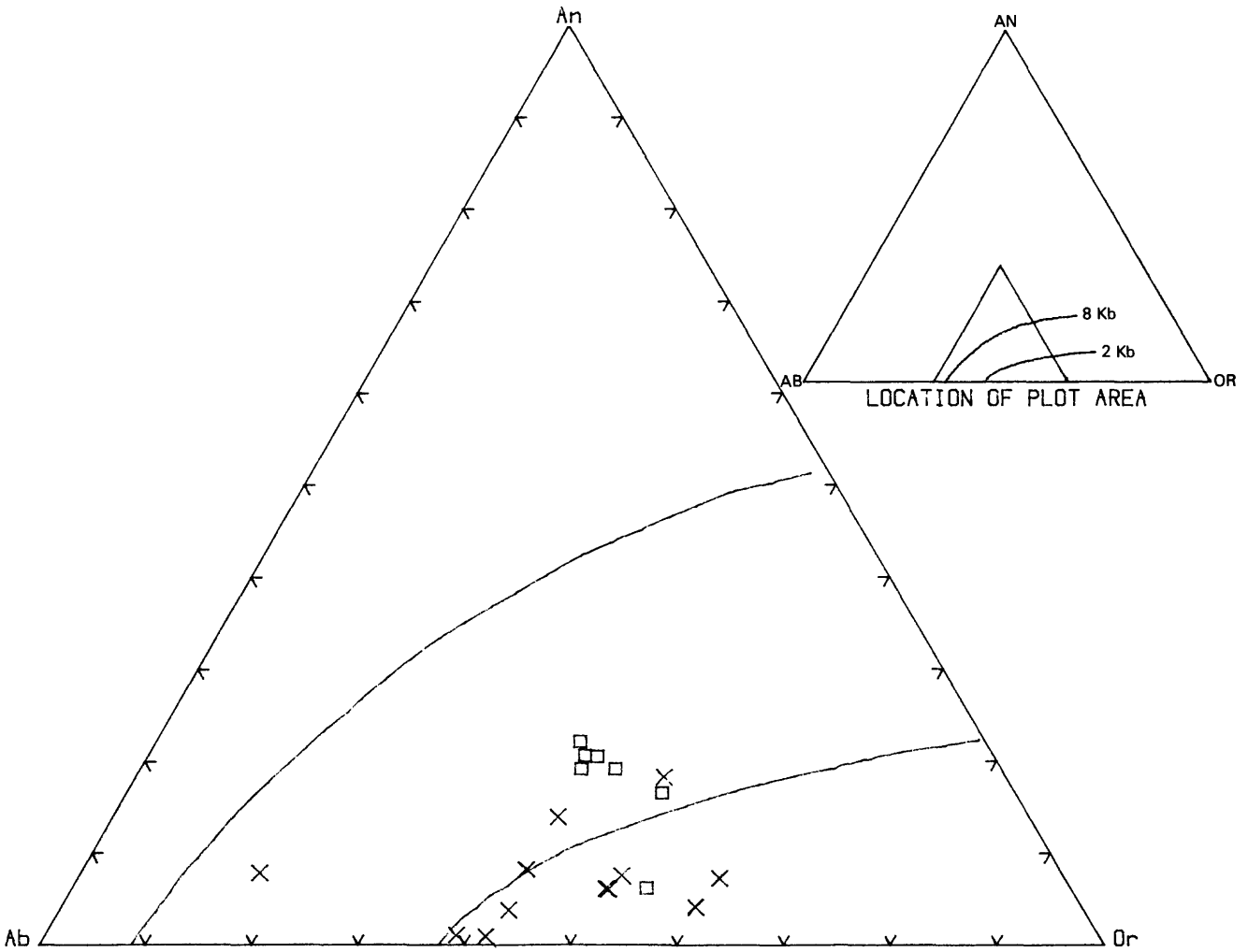

Figure 3.—Ternary diagram showing the normative composition of granitic samples from Ba'gham and the water-saturated eutectic composition at 2 and 8 kilobars (Whitney, 1975). Data for hypersolvus granite are shown by X and for subsolvus granite by squares.

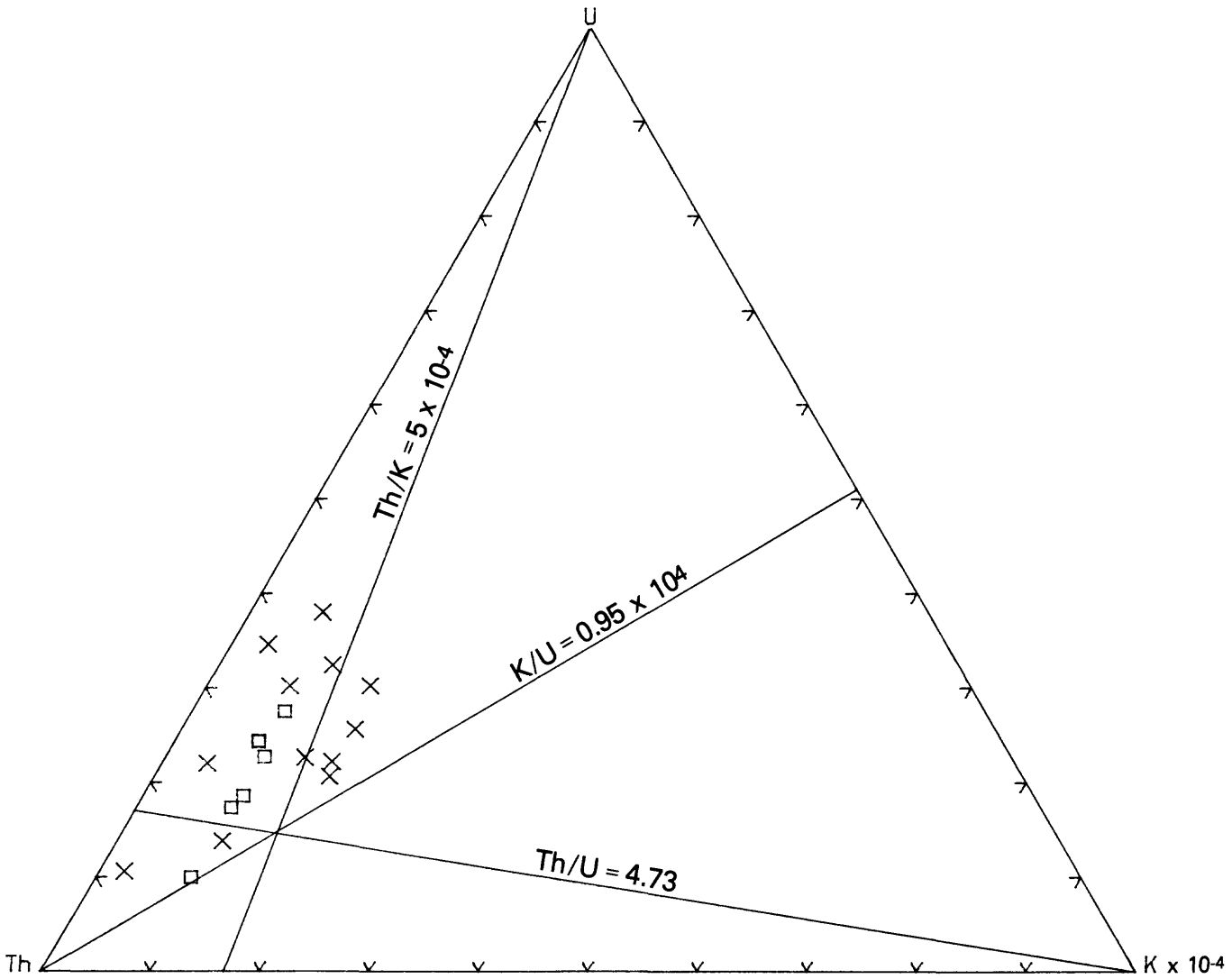

Figure 4.--Ternary diagram showing the relative proportions of uranium, thorium, and potassium relative to average granite (Stuckless and VanTrump, 1982). Data for hypersolvus granite are shown by X and for subsolvus granite by squares.

There is a suggestion in the areal pattern generated by the trace-element data that at least some of the apparent high degree of petrologic evolution is due to hydrothermal activity. Both uranium and thorium contents are anomalously high in apparently unmineralized rock near the areas of very high radioactivity. Furthermore, the anomalous uranium values are spread over a much larger area than the anomalous thorium values and occur within both the Ba'gham and Jufayfah granites (fig. 5). However, there are no obvious indications of hydrothermal alteration in the intervening septum of volcanic rocks.

There are not enough data points to accurately contour the trace-element contents around the anomalous radioactivity at Ba'gham. However, it appears that the anomalous values for niobium (>100 ppm), yttrium (>100 ppm), and thorium (>39.23 ppm) are restricted to the hypersolvus granite. Samples of this granite also have the highest rubidium contents (>300 ppm), but somewhat elevated values (>200 ppm) for rubidium continue across the contact and into the subsolvus granite. These relations are shown schematically on figure 6. The pattern is consistent with an origin through hydrothermal activity that was most intense near the strong radioactive anomalies. Pervasive alteration around this center resulted in a halo effect such that the most geologically mobile elements (Rb and U) exhibit the largest halo and the most insoluble element (Th) exhibits the smallest.

Economic considerations

Each of the areas of anomalous radioactivity visited was characterized by broken and sheared rock that appeared to be physically disaggregated by weathering. Several areas were cut by thin quartz veins, and most areas were distinctly redder than those with background levels of radioactivity. In most cases, the anomalous radioactivity was restricted to less than 100 m^2, and the transitions between highest and only moderate levels of radioactivity was fairly sharp (within a few meters). The highest levels of radioactivity seemed to follow an elonate podlike pattern. These features are very similar to those described for Bokan Mountain, Alaska (Staatz and others, 1980).

No truly fresh samples of anomalously radioactive material could be obtained. Samples dug out of the rock with a pick had the appearance of grus. Analyses of these samples and strongly decomposed but unmineralized granite are presented in table 5. The data show that, in all but one sample, thorium is the dominant radioactive element. An original high uranium content or a possible enrichment of uranium at depth cannot be ruled out because of the poor physical state of the samples and the high mobility of hexavalent uranium in the near-surface environment. However, the small size of the thorium anomalies and their discontinuous nature suggest that even moderate uranium concentrations ($\sim$5000 ppm) at depth would not produce an economic deposit.

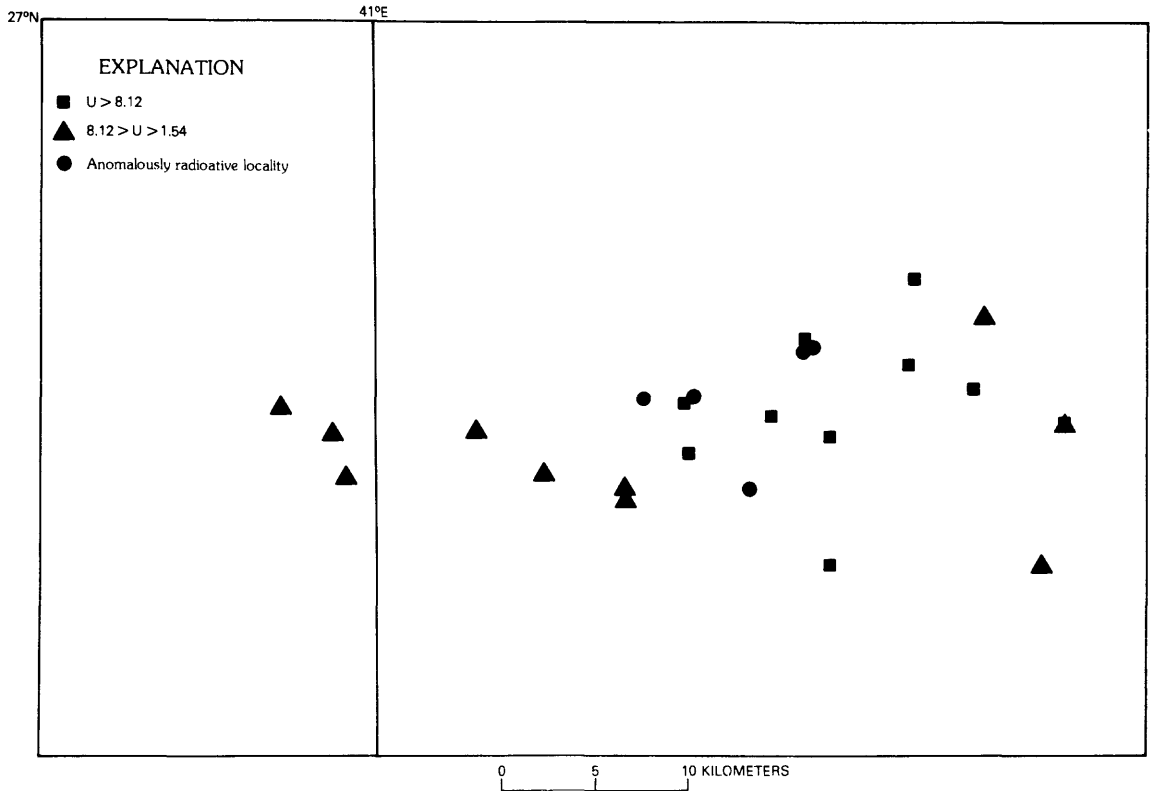

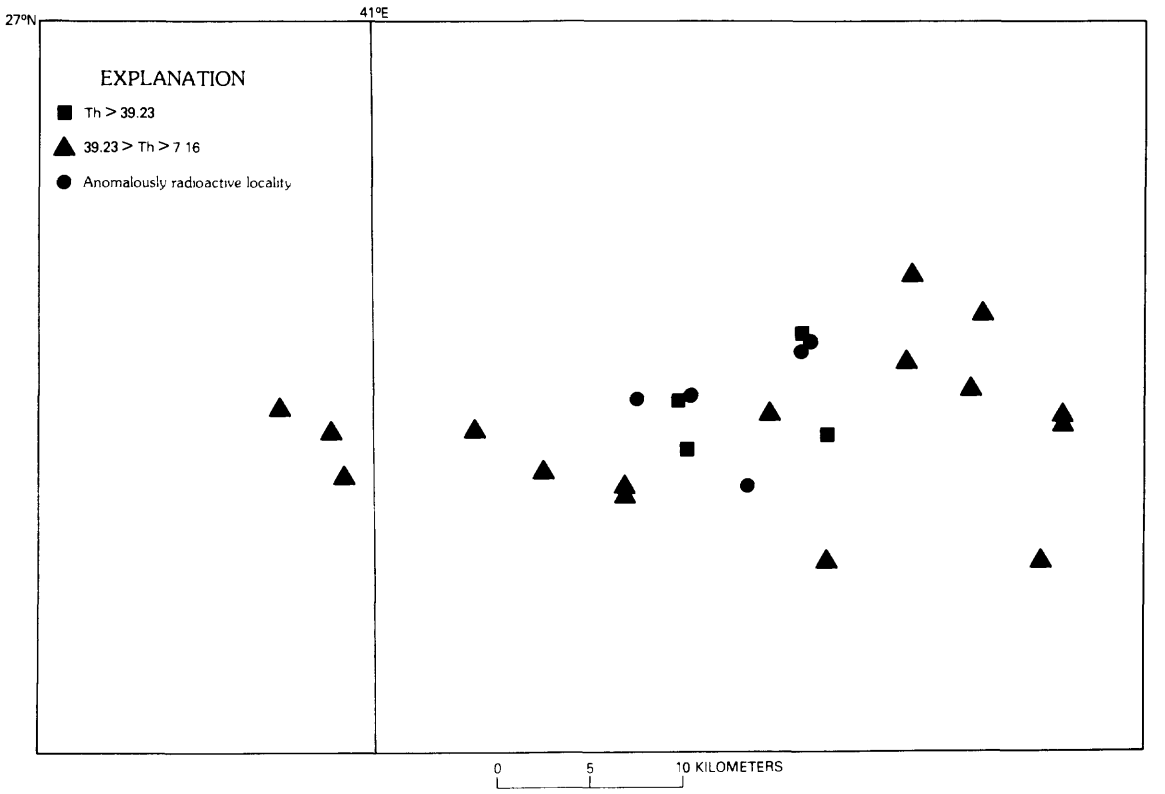

Figure 5.—Maps showing the concentrations of uranium (top) and thorium (bottom) in the Ba'gham area. Symbols represent a comarrison to average granite such that data points with values that exceed the mean plus one standard deviation (Stuckless and Van Trump, 1982) are shown by squares.

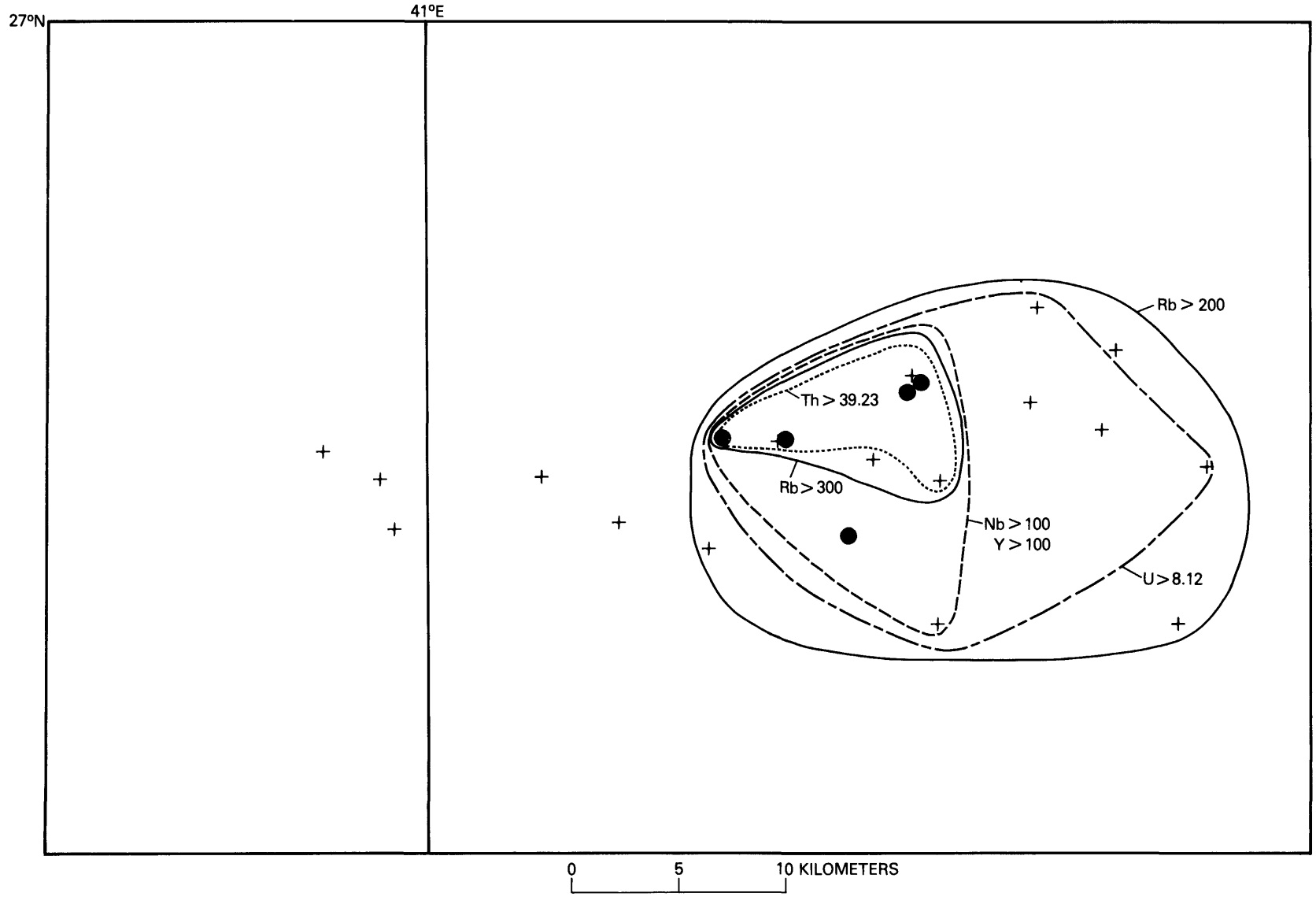

Figure 6.—Schematic map showing areas of relative trace-element enrichment. Areas of anomalous radioactivity are shown by dots, and sample localities are shown by pluses.

Table 5.--Radioelement concentrations for physically decomposed samples of granite and vein material
[Analysts: U, R. B. Vaughn; RaeU, eTh, and eK, C. A. Bush.]

Sample Number	U (ppm)	RaeU (ppm)	eTn (ppm)	eK (wt %)
155194 A	1040	780	1158	5.86
155195	1250	1260	1190	3.60
155197 A	572	550	25900	--
155197 B	50.4	37.3	1380	4.64
155199	1980	4900	150000	--
155200	6.5	4.0	32.9	3.78
155212	60.3	36	1460	2.9

155194 A - is a sample of decomposed quartz vein and granophyre from 26°56'24" N. and 40°54'43" E.

155195 - is a sample of red, pervasively altered and decomposed granite from 26°56'20" N. and 40°56'43" E.

155197 A - is a sample of crushed, thin veins of jasperlike material from 26°55'48" N. and 40°56'06" E.

155197 B - is a sample of decomposed coarse-grained granite that is bleached white on the surface and stained red at depth from 26°55'48" N. and 40°56'06" E.

155199 - is a sample of crushed jasperlike vein material from 26°55'48" N. and 40°56'46" E.

155200 - is a sample of coarse-grained decomposed granite from 26°55'41" N. and 41°01'08" E.

155212 - is a sample of coarse-grained decomposed granite with abundant fine-grained veins from 26°54'50" N. and 40°55'23" E.

Several radioactive granites have been proposed as the source material for low-temperature to moderate-temperature uranium deposits (for example, Rosholt and others, 1973; Von Backstrom, 1974; Stuckless, Troeng, and others, 1982). Lead-isotope studies have been used to demonstrate the loss of uranium from apparently fresh samples of granite (Stuckless and Nkomo, 1978). These studies have shown that the amount of uranium lost exceeds the known amount of nearby uranium ore by factors of more than 100 and that the timing of uranium loss coincides with the time of uranium-ore deposition. The poor physical state of samples from Ba'gham precludes the use of lead isotopes because of the low probability that lead was not mobilized; however, other features noted for proposed uranium source rocks can be compared to the data for samples from Ba'gham.

Stuckless and Ferreira (1976) and Rosholt (1983) have noted that the mobilization of uranium is largely due to interaction of water and uranium along grain boundaries and cleavage planes and that, if much uranium is located in such sites, intermediate daughter products are rapidly mobilized such that a disequilibrium develops within the ^{238}U decay chain. Daughter products such as ^{226}Ra are not compatible with the crystal chemistry of these sites, and, therefore, if these sites are in contact with water, RaeU values are low relative to chemical uranium values, and the two values do not correlate well. This type of disequilibrium is noted at Ba'gham (fig. 7), and thus some secondary uranium deposits may exist if a favorable trap for the mobilized uranium was available. The volume of favorable source rock is small relative to other well-studied areas, and the sedimentary trap would therefore have to be small and very efficient in order to create an economic deposit. Uranium deposits such as the calcrete deposits of Western Australia have apparently developed from granitic source rocks that have lost only small amounts of uranium (Stuckless and others, 1981).

Although the mineralization at Ba'gham does not appear to be economic, the data obtained may be useful in the search for similar but larger deposits. The large halo effect noted for uranium and rubidium may provide a subtle indication of nearby concentrations of rare elements. Rubidium may be particularly useful in cases where the elements of economic interest (such as rare earths, niobium, and tantalum) have been concentrated without a concomitant increase in the radioelements (which could be located from aeroradiometric surveys). In this regard, drilling at Ba'gham may provide some useful data as well as a check for higher concentrations at depth.

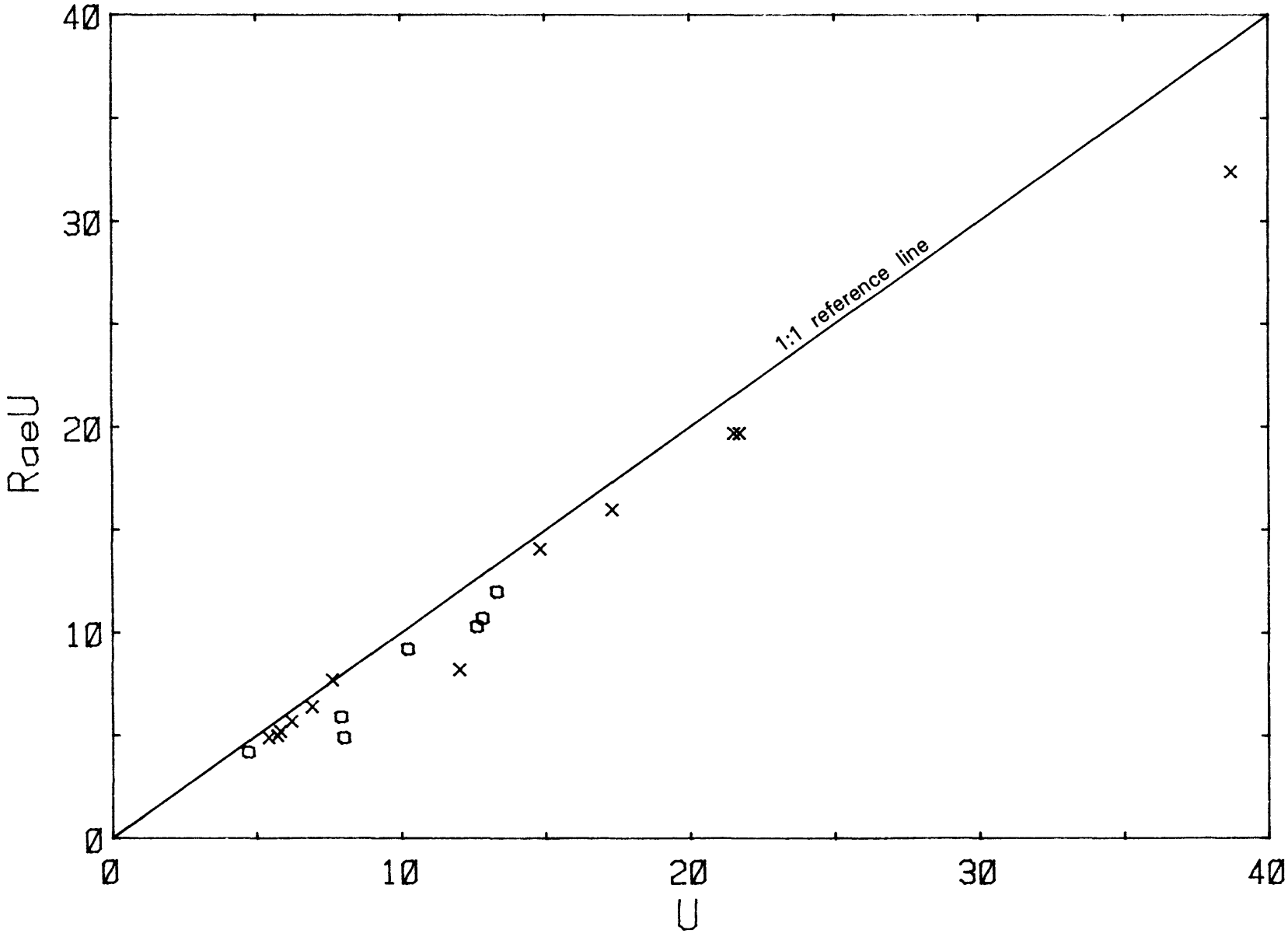

Figure 7.—Plot of radium-equvalent uranium (RaeU) versus uranium (U). Data for hypersolvus granite are shown by X and for subsolvus granite by squares.

Geochronology

Whole-rock Rb-Sr isochrons were attempted for both the hypersolvus and subsolvus granites (table 4). The range of values obtained for the subsolvus granite is small relative to analytical error for individual samples, and the resulting isochron is therefore poorly constrained such that calculated errors for age and intercept are large. A regressed line through the data points yields a slope of 0.009388 ± 0.001350 and an intercept of 0.6939 ± 0.0114 (errors at the 95-percent confidence level). The corresponding age is 658 ± 92 m.y.

The extremely low initial $^{87}Sr/^{86}Sr$ value indicates that the Rb-Sr system has not remained closed from the time of intrusion of the granite until the present. Addition of rubidium and (or) loss of strontium at some postintrusive time seems likely. All of the subsolvus samples contain sericite as an alteration product of feldspar. Strontium would be lost in preference to rubidium during this alteration. The areal distribution of trace-element contents suggests that rubidium may have been added to the subsolvus granite at the time when hydrothermal alteration created the radioactive anomalies. If either rubidium addition or strontium loss postdated intrusion of the subsolvus granite, the apparent initial $^{87}Sr/^{86}Sr$ value would be too low, and the apparent age would be inaccurate. In fact, data points for the subsolvus granite fall on the isochron for the hypersolvus granite within the limits of analytical error (fig. 8), and therefore, the relative ages of the two plutons are not resolvable with the Rb-Sr system.

Data for the hypersolvus granite yield a good isochron (fig. 8) with a line fit within the limits of analytical error (MSWD=0.93). The regressed line has a slope of 0.008560 ± 0.000103 and an intercept of 0.7018 ± 0.0017. The corresponding age is 600 ± 7 m.y., which is near the middle of the period of posttectonic plutonism cited as typical for the Arabian Shield (Schmidt and Brown, in press). However, the age is slightly older (by about 20 m.y.) than ages for other postorogenic plutons in the northern part of the shield (J. S. Stuckless and C. E. Hedge, unpublished data), and the initial $^{87}Sr/^{86}Sr$ value is low (by about 0.0012) relative to available data (Fleck and Hadley, in press; J. S. Stuckless and C. E. Hedge, unpublished data). Although these small differences are not statistically significant, they may suggest minor perturbations of the isotopic systematics by hydrothermal alteration very shortly after intrusion.

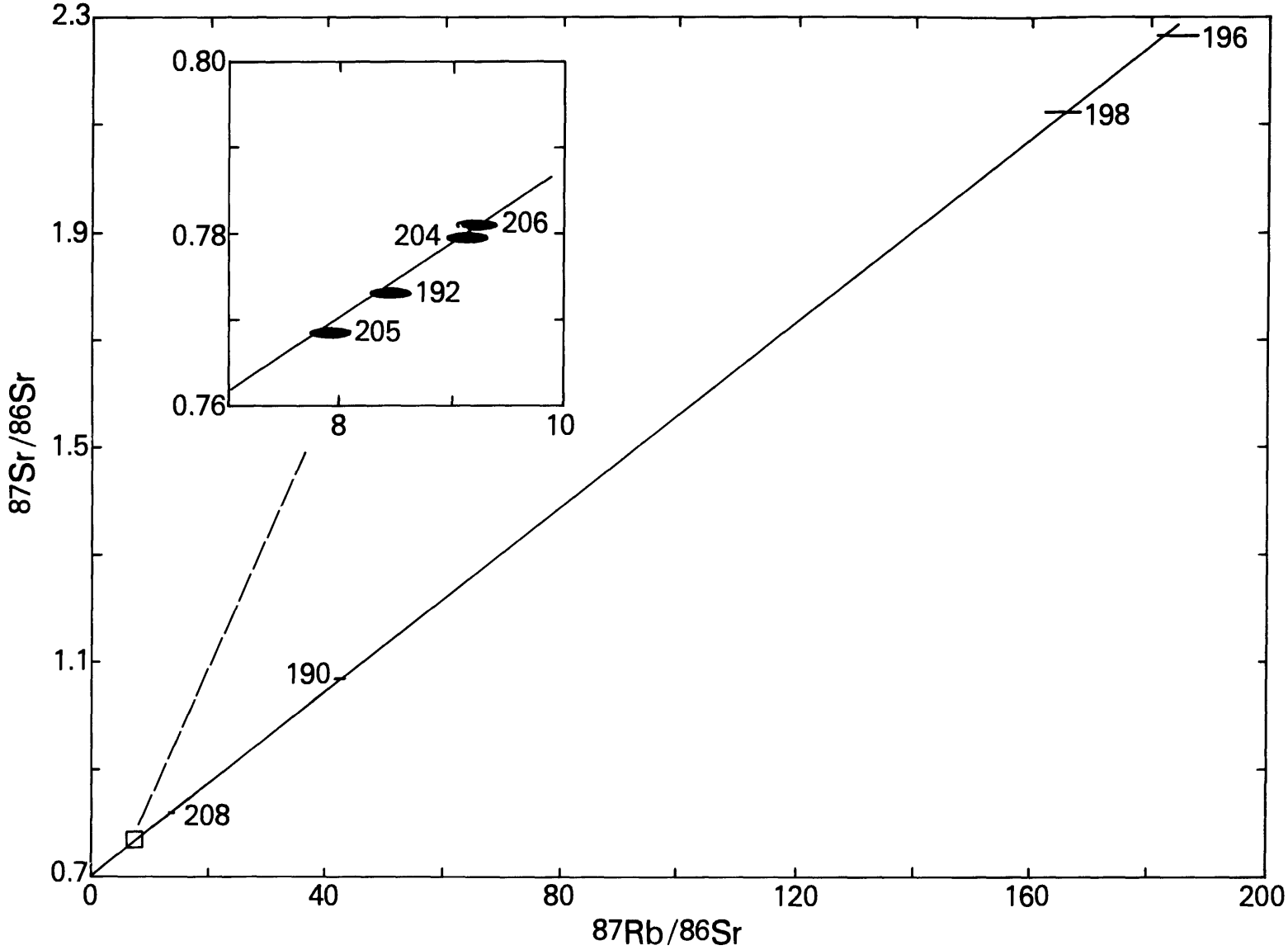

Figure 8.—Rb-Sr isochron plot for granite samples from Ba'gham, Kingdom of Saudi Arabia. Symbol size represents analytical error at the 95-percent level of confidence. Data for the hypersolvus granite are shown in the inset relative to the isochron for the hypersolvus granite. The calculated age for the hypersolvus granite is 600+7 Ma. Sample numbers are last three digits of the sample numbers listed in table 4.

SUMMARY

Anomalous radioactivity near Ba'gham is restricted to areas underlain by a 600-m.y.-old postorogenic granite. The granite is geochemically similar to other postorogenic granites of the northern Arabian Shield, but exhibits features consistent with a higher degree of chemical evolution, such as a low average K/Rb value and a high average Rb/Sr value. The granite is hypersolvus and has features similar to the peralkaline clan, such as elevated contents of iron, niobium, and zirconium, but is chemically metaluminous to weakly peraluminous.

Average contents of uranium and thorium are enriched relative to other postorogenic granites of the Arabian Shield and to world-average granite. However, average contents of these elements are a factor of 20 below economic grade. Pronounced radioactive anomalies are small in areal extent and are dominated by thorium. The advanced stage of physical disintegration of surface materials and the probable mobilization of any uranium associated with thorium allow for possible concentrations of uranium at depth and for possible secondary deposits near Ba'gham if suitable chemical traps existed at the time of uranium mobilization. However, it is likely that either type of uranium deposit would be small.

There is a distinct halo effect for several trace elements around the area that contains the thorium anomalies. The halos are largest for the elements with the greatest geochemical mobility and seem to extend beyond the boundary of the hypersolvus granite. This condition is particularly true for rubidium in that the Rb-Sr isotope systematics have been disturbed for samples of the subsolvus granite at a distance of several kilometers from the contact with the younger granite. The halos are interpreted to have been caused by the hydrothermal activity centered near the radioactive anomalies. If this interpretation is correct, the identification of similar halos may provide a guide to exploration for deposits that lack surficial expression.

The anomaly at Ba'gham is similar in many aspects to the uranium and thorium deposit at Bokan Mountain, Alaska. Neither deposit is economic at this time (although both uranium and thorium have been produced at Bokan Mountain), and neither deposit contains abundant carbonate material. However, peralkaline granites are widely distributed throughout the Arabian Shield, and it seems possible that elsewhere one or more of these anomalously radioactive granites could be associated with carbonatites that would increase the chances of forming an economic uranium, thorium, and rare-earth deposit.

DATA STORAGE

Data-file USGS-DF-04-21 (Stuckless and others, 1984) has been established for the storage of data used in this report.

No entries or updates have been made to the Mineral Occurrence Documentation System (MODS) data bank.

REFERENCES CITED

Armbrustmacher, T. J., 1979, Replacement and primary magmatic carbonatites from the Wet Mountains area, Fremont and Custer Counties, Colorado: Economic Geology, v. 74, p. 888-901.

Bunker, C. M., and Bush, C. A., 1966, Uranium, thorium, and radium analyses by gamma-ray spectrometry (0.184-0.352 million electron bolts), in Geological Survey research 1966: U.S. Geological Survey Professional Paper 550-B, p. B176-B181.

————1967, A comparison of potassium analyses by gamma-ray spectrometry and other techniques, in Geological Survey research 1967: U.S. Geological Survey Professional Paper 575-B, p. B164-B169.

Chevremont, P., 1982, Geologic and mineral reconnaissance of the volcanosedimentary and mafic plutonic rocks in the Ha'il area: Saudi Arabian Deputy Ministry for Mineral Resources Open-File Report BRGM-OF-02-39, 33 p.

Delfour, J., 1977, Geology of the Nuqrah quadrangle, sheet 25E, Kingdom of Saudi Arabia: Saudi Arabian Directorate General of Mineral Resources Geologic Map GM-28, 32 p., scale 1:250,000.

Elliott, J. E., 1983, Peralkaline and peraluminous granites and related mineral deposits of the Arabian Shield, Kingdom of Saudi Arabia: Saudi Arabian Deputy Ministry for Mineral Resources Open- File Report USGS-OF-03-56, 37 p. also, 1983, U.S. Geological Survey Open-File Report 83-389.

Felsche, J., and Hermann, A. G., 1978, Yttrium and lanthanides, chapter 39, in Wedepohl, K. H., ed., Handbook of Geochemistry: Verlin, Springer-Verlag, v. 2, no. 5, p. 57-71.

Fleck, R. J., and Hadley, D. G., in press Ages and strontium initial ratios of plutonic rocks in a transect of the Arabian Shield: Journal of the Geological Society of London.

Harris, N. B. W., and Marriner, G. F., 1980, Geochemistry and petrogenesis of a peralkaline granite complex from the Midian Mountains, Saudi Arabia: Lithos, v. 13, p. 325-337.

Kellogg, K. S., 1983, Reconnaissance geology of the Qufar quadrangle, sheet 27/41 D, Kingdom of Saudi Arabia: Saudi Arabian Deputy Ministry for Mineral Resources Open-File Report USGS-OF-04-2, 35 p.; also, 1984, U.S. Geological Survey Open-File Report 84-150.

Krauskopf, K. B., 1967, Introduction to geochemistry: New York, McGraw-Hill, 721 p.

Luth, W. C., Jahns, R. H., and Tuttle, O. F., 1967, The granite system at pressures of 4 to 10 kilobars: Journal of Geophysical Research, v. 69, p. 759-773.

Mathews, G. W., 1978, Uranium occurrences in and related to igneous rocks, in Geologic characteristics of environments favorable for uranium deposits: U.S. Department of Energy Open-File GJBX-67(78), p. 121-180.

Millard, H. T., Jr., 1976, Determination of uranium and thorium in U.S. Geological Survey standard rocks by the delayed neutron technique, in Flanigan F. J., ed., Descriptions and analyses of eight new USGS rock standards: U.S. Geological Survey Professional Paper 840, p. 61-65.

Olson, J. C., Marvin, R. F., Parker, R. L., and Mehnert, H. H., 1977, Age and tectonic setting of lower Paleozoic alkalic and mafic rocks, carbonatites,, and thorium veins in south-central Colorado: U.S. Geological Survey Journal of Research, v. 5, p. 673-687.

Olson, J. C., Shawe, P. R., Pray, L. C., and Sharp, W. N., 1954, Rare-earth deposits of the Mountain Pass district, San Bernardino County, California: U.S. Geological Survey Professional Paper 261, 75 p.

Quick, J. E., 1983, Reconnaissance geology of the Ghazzalah quadrangle, sheet 26/41 A, Kingdom of Saudi Arabia: Saudi Arabian Deputy Ministry for Mineral Resources Open-File Report USGS- OF-03-91, 44 p.; also, 1983, U.S. Geological Survey Open-File Report 83-331.

————1984, Reconnaissance geology of the Zarghat quadrangle, sheet 26/40 B, Kingdom of Saudi Arabia: Saudi Arabian Deputy Ministry for Mineral Resources Open-File Report USGS-OF-04-28, 37 p.; also, 1984, U.S. Geological Survey Open-File Report

Rosholt, J. N., 1983, The isotopic composition of uranium and thorium in crystalline rocks: Journal of Geophysical Research, v. 88 p. 7315-7330.

Rosholt, J. N., Zartman, R., E., and Nkomo, I. T., 1973, Lead isotope systematics and uranium depletion in the Granite Mountains, Wyoming: Geological Society of America Bulletin, v. 84, p. 989-1002.

Schmidt, D. L., and Brown, G. F., *in press*, Major-element chemical evolution of the late Proterozoic shield of Saudi Arabia: The First Symposium of Pan African Crustal Evolution in the Arabian-Nubian Shield, IGCP Project 164.

Shand, S. J., 1951, Eruptive rocks--their genesis, classification, and their relation to ore deposits (4th ed.): New York, John Wiley, 488 p.

Staatz, M. H., Hall, R. B., Macke, D. L., Armbrustmacher, T. J., and Brownfield, I. K., 1980, Thorium resources of selected regions in the United States: U.S. Geological Survey Circular 824, 32 p.

Steiger, R. H., and Jaeger, E., 1977, Subcommission on geochronology: convention on the use of decay constants in geo- and cosmo- chronology: Earth and Planetary Science Letters, v. 36, p. 359-367.

Streckeisen, A. L., 1976, To each plutonic rock its proper name: Earth-Science Reviews, v. 12, p. 1-33.

Stuckless, J. S., Bunting, J. A., and Nkomo, I. T., 1981, U-Th-Pb systematics of some granitoids from the northeastern Yilgarn Block, Western Australia and implications for uranium source rock potential: Journal of the Geological Society of Australia, v. 28, p. 365-375.

Stuckless, J. S., and Ferreira, C. P., 1976, Labile uranium in granitic rocks: International Atomic Energy Agency, International Symposium on Exploration of Uranium Ore Deposits, Vienna, 1976, Proceedings, p. 717-730.

Stuckless, J. S., Knight, R. J., VanTrump, George, Jr., and Budahn, J. R., 1982, Trace-element geochemistry of postorogenic granites from the northeastern Arabian Shield, Kingdom of Saudi Arabia: Saudi Arabian Deputy Ministry for Mineral Resources Open-File Report USGS-OF-02-91, 34 p.; also, 1983, U.S. Geological Survey Open-File Report 83-287.

Stuckless, J. S., and Nkomo, I. T., 1978, Uranium-lead isotope systematics in uraniferous alkali-rich granites from the Granite Mountains, Wyoming: implications for uranium source rocks: Economic Geology, v. 73, p. 427-441.

Stuckless, J. S., Troeng, B., Hedge, C. E., Simmons, K., and Nkomo, I. T., 1982, Age of uranium mineralization at Lilljuthatten in Sweden and constraints on ore genesis: Sveriges Geologiska Undersokning, C789, 49 p.

Stuckless, J. S., and VanTrump, George, Jr., 1979, A revised version of Graphic Normative Analysis Program (GNAP) with examples of petrologic problem solving: U.S. Geological Survey Open-File Report 79-1327, 115 p.

_____1982, A compilation of radioelement concentrations in granitic rocks of the contiguous United States: International Atomic Energy Agency/DECD Symposium on Uranium Exploration Methods, Vienna, 1982, Proceedings, p. 198-208.

Stuckless, J. S., VanTrump, George, Jr., Bunker, C. M., and Bush, C. A., *in press*, Preliminary report on the geochemistry and uranium favorability of the postorogenic granites of the northeastern Arabian Shield, Kingdom of Saudi Arabia: Proceedings, Pan-African Crustal Evolution in Arabia and northeast Africa, IGCP Project 164.

Stuckless, J. S., Quick, J. E., and VanTrump, George, Jr., 1984, Supporting data for geochemical investigations and assessment of anomalous radioactivity at Ba'gham, Kingdom of Saudi Arabia: Available from Saudi Arabian Deputy Ministry for Mineral Resources Data-File USGS-DF-04-21.

Taggart, J. E., Jr., Lichte, F. E., and Wahlberg, J. S., 1982, Methods of analysis of samples using X-ray fluorescence and induction- coupled plasma spectrometry, in Lipman, P. W., and Mullineaux, D. R., eds., The 1980 eruption of Mount St. Helens, Washington: U.S. Geological Survey Professional Paper 1250, p. 683-687.

Thornton, C. P., and Tuttle, O. F., 1960, Chemistry of igneous rocks. I. Differentiation index: American Journal of Science, v. 258, p. 664-684.

Tuttle, O. F., and Bowen, N. L., 1958, Origin of granite in the light of experimental studies in the system $NaAlsi_3O_8$-$KAlSi_3O_8$-SiO_2-H_2O: Geological Society of America Memoir 74, 153 p.

VanTrump, George, Jr., and Miesch, A. T., 1977, The U.S. Geological Survey RASS-STATPAC system for management and statistical reduction of geochemical data: Computer and Geoscience, v. 3, p. 475-488.

Von Backstrom, J. W., 1974, Other uranium deposits, in Formation of uranium ore deposits: International Atomic Energy Agency, Vienna, p. 605-624.

Whitney, J. A., 1975, The effects of pressure, temperature, and XH_2O on phase assemblage in four synthetic rock compositions: Journal of Geology, v. 83, p. 1-31.

York, Derek, 1969, Least-squares fitting of a straight line with correlated errors: Earth and Planetary Science Letters, v. 5, p. 320-324.